Nano Progress

Ariviyal Publishing

Research Article

DOI: 10.36686/Ariviyal.NP.2021.03.06.033

Nano Prog., (2021) 3(6), 51-59.

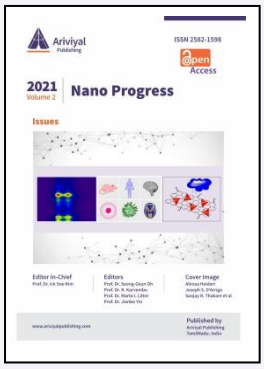

Nano - Glass Waste Substitution for Portland cement Pastes

H. H. M. Darweesh

Refractories, Ceramics and Building Materials Department, National Research Centre, Cairo, Egypt.

***Corresponding author E-mail address**: hassandarweesh2000@yahoo.com (H. H. M. Darweesh)

ISSN: 2582-1598

Crossref

Publication details
Received: 29th July 2021
Revised: 27th October 2021
Accepted: 27th October 2021
Published: 17th November 2021

Abstract: The effect of glass waste (GW) substitution on physical, chemical and mechanical properties of Portland cement pastes (OPC) was investigated. The results generally showed that as the GW content increased in the cement batch, the fineness of the whole cement batches increased too. All cement characteristics improved and enhanced as the hydration time proceeded up to 90 days. The water of consistency and setting times (initial and final) decreased with GW content due to the presence of sodium lignosulphonate superplasticizer, which accelerated the setting of cement pastes. The heat of hydration, combined water, bulk density and compressive strength were improved and enhanced with the increase of GW content only up to 12 wt% (G4), whereas the free lime and apparent porosity decreased. With > 12 wt% GW (G5-G7), the heat of hydration, combined water, bulk density and compressive strength were shortened and decreased at all hydration stages, while the free lime and apparent porosity increased. The optimum content of GW was 12 wt%, which achieved the best results, and that containing 21 wt% GW exhibited the lowest, but still higher than those of the blank at all hydration ages. The SEM microscopy showed the formation of ettringite phase ($C_3A.\ 3CaSO_4.\ 32\ H_2O$), sheets and blocks of CSH in G0, G2 and G4, respectively.

Keywords: Cement; Glass waste; setting times; heat of hydration; free lime; density; porosity; strength; SEM

1. Introduction

The increase in the various solid waste residues in the cities particularly those do not decompose easily neither in nature, nor by weathering factors for thousands of years such as wastes of glass bottle that created the growth of both ground and air populations. The recycling of these wastes is an important environmental and economical alternative solution.[1–10] Glass wastes are being non-biodegradable in nature, glass disposal as landfill has environmental impacts and also could be expensive. Though the cement or concrete is the prime construction material worldwide, it has adverse impacts on the environment.[11] Cement industry is a major source of greenhouse gas emissions.[12] So, the use of supplementary cementitious materials to offset a portion of the cement in concrete is a promising solution to reduce these environmental impacts from the industry. Many industrial wastes have been used successfully as supplementary cementitious materials. Some of these materials are silica fume,[13,14] granulated blast furnace slag,[13-15] fly ash,[13,14] Homra,[16] sugarcane bagasse ash.[12,17-19] These materials are used to create blended cements which can improve workability, durability, early and long term strength, and also economy.[20] Researches indicated that the glass powder has the same chemical and phase composition of the traditional afore materials, and therefore, it can behave alike.[21-24] Glass waste is very abundant, of no or low economic value and it is often land filled.[25] The conversion of glass to micro-or nanosized particles, improves and enhances the reactions between glass particles and the hydrates of cement. This can bring minor energy, environmental and economic benefits when cement is partially substituted with the milled glass waste to produce cement and/or concrete.[12] Several studies focused on the use of glass waste as fine or coarse aggregates in concrete production.[12,26] This can be achieved by using a grinding operation with the help of ‘‘Ball Mill” which is generally used in cement industry to grind cement clinker. Rashed, 2014; Nassar and Soroushian, 2011[12,27] stated that the glass addition was not conclusive considering workability and strength, while the chloride resistance was found to be similar with those of the control. Utilization of waste glass in ceramic and brick manufacturing process also was discussed in many recent studies.[1,28-31]

The main objective of the current study is to evaluate the effect of glass waste substitution on the physic-mechanical properties and microstructure of Portland cement pastes. The obtained results are confirmed by SEM microscopy for some selected samples.

Table 1. Composisition of the used raw materials, mass %.

Oxide / Material	SiO_2	Al_2O_3	Fe_2O_3	CaO	MgO	MnO	SO_3	Na_2O	P_2O_5	K_2O	LOI
OPC	20.12	4.25	1.29	63.13	1.53	0.36	2.54	0.55	0.19	0.30	2.64
GW	70.31	2.46	0.26	8.69	3.62	0.02	----	12.52	----	1.06	----

Table 2. Mineralogical composition of the used OPC sample, mass %.

Phase / Material	C_3S	β-C_2S	C_3A	C_4AF
OPC	43.01	30.00	5.65	9.58

Fig. 1. Glass waste powder nanoparticles.

2. Experimental Section

2.1. Raw materials

The used raw materials in the current research study are Ordinary Portland cement (OPC Type I- CEM I 42,5R) with blaine surface area 3400 cm^2/g, and glass waste (GW) as a source of nanosilica with fineness 6810 cm^2/g (Fig. 1). The Blaine surface area was applied by the "Air Permeability Apparatus". The OPC was supplied from Sakkara cement factory, Giza, Egypt, and its commercial name is known as "Asmant El-Momtaz", while GW sample was provided from a local factory for glass, Giza, Egypt. The chemical composition of the OPC and GW measured by X-ray florescence technique (XRF) is shown in Table 1. The mineralogical phase composition of the used OPC as calculated from Bogue equations[32,33] is given in Table 2, while the mix composition is illustrated in Table 3. The GW particles are amorphous and crystalline and it is mainly composed of a large percentage of nano-SiO_2 and a lower percentage of nano-Al_2O_3.

2.2. Physical properties

The physical properties[32-35] of the OPC and GW are calculated from the following relations:

$$Kb = CaO + MgO / SiO_2 + Al_2O_3 \quad (1)$$

$$Hm = CaO / SiO_2 + Al_2O_3 + Fe_2O_3 \quad (2)$$

$$Sm = SiO_2 / Al_2O_3 + Fe_2O_3 \quad (3)$$

$$Am = Al_2O_3 / Fe_2O_3 \quad (4)$$

$$Lm = 100 \times CaO / 2.8 \times SiO_2 + 1.1 \times Al_2O_3 + 0.7 \times Fe_2O_3 \quad (5)$$

Where, Kb, Hm, Sm, Am and Lm are the basicity coefficient, hydration modulus, SiO_2 modulus, Al_2O_3 modulus and CaO modulus, respectively.

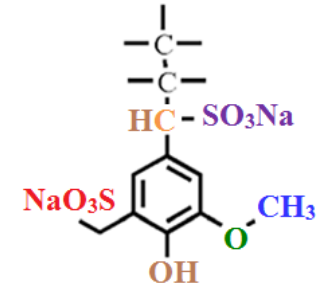

Fig. 2. The chemical structure of sodium lignosulphonate.

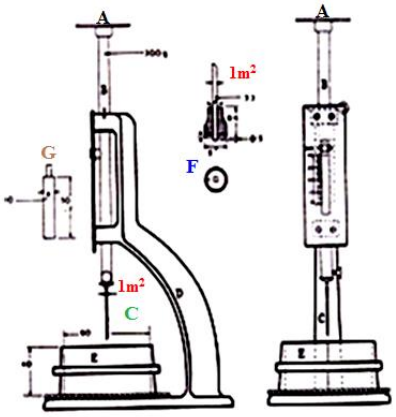

Fig. 3. Vicat Apparatus for water consistency and setting times

2.3. Preparation and methods

There are eight cement batches from OPC and GW as 100:0, 97:3, 94:6, 91:9, 88:12, 85:15, 82: 18 and 79:21 having the symbols: G0, G1, G2, G3, G4, G5, G6 and F7, respectively. The blending process was mechanically made in a porcelain ball mill containing three balls for one hour to assure the complete homogeneity of all batches. Before casting of cement cubes, all moulds were oiled with a thin film of motor engine oil, to facilitate the release of the cubes from the moulds during the de-moulding. In order to improve the dispersion of the different cement batches, a certain percentage of Na-lignosulphonate admixtures must be added to all cement mixtures with the mixing water during casting of cement pastes to avoid the agglomeration of the nanoparticles of cement powder and GW.[36] Sodium lignosulfonate admixture (SLA) was applied due to its higher activity than other conventional ones (Fig. 2).

A mechanical mixing was used for all cement mixtures using a suitable laboratory mechanical mixer in order to obtain homogenous mixtures. Firstly, the standard water of consistency[37] and setting time[38] of the various cement pastes were directly determined using Vicat Apparatus (Fig. 3).

The water of consistency could be determined from the following relation:

$$WC, \% = A / C \times 100 \quad (6)$$

Table 3. The batch composition of cement mixtures, mass %.

Batch Material	G0	G1	G2	G3	G4	G5	G6	G7	Density, g/cm^3	Blaine Finenes, cm^2/g	Specific gravity
OPC	100	97	94	91	88	85	82	79	2.2215	3400	3.14
GW	----	3	6	9	12	15	18	21	2.6546	6810	3.31
Fineness, cm^2/g	3400	3485	3630	3785	3855	4100	4325	4565			

Where, A is the amount of water taken to produce a suitable paste, C is the amount of cement mix (300 g). The initial setting time was measured by calculating the time taken from the moment at which the needle could penetrate to the paste up to 5 ml from the bottom, while the final setting time was calculated by measuring the time taken from the moment at which the water added to the cement till the final set when the impression of the needle disappeared on the surface of the pastes.

During the dry mixing process, the right w/c-ratio was poured into the cement portion inside the mixer and then run the mixer for about 10 minutes at an average speed of 10 rpm in order to have a perfect homogenous mixture. During casting of the cement cube moulds, each already prepared oil mould was filled with the premixed cement composite and rammed 10 minutes to remove all air bubbles tapped within the mixture. The moulds were filled to the top surface and smoothed with a flat stainless steel trowel or spatula to obtain a flat and smooth surface. The cement pastes were then cast using the predetermined water of consistency, moulded into one inch cubic stainless steel moulds (2.5 x 2.5 x 2.5 cm^3) using about 500 g cement mix, vibrated manually for three minutes and then on a mechanical vibrator for another three minutes. The surface of the moulds was smoothed using a suitable trowel or spatula. After casting all cement cubes, they were covered with a black wet sheet for the first 24 hours to prevent moisture loss. Thereafter, the moulds were kept in a humidity chamber for 24 hours under 100% relative humidity and room temperature 23 ± 1°C. In the following day, it demoulded and soon cured in water till the time of testing at 1, 3, 7, 28 and 90 days.

At each hydrating interval, the bulk density (BD) and apparent porosity (AP) of the hardened cement pastes[32,39-41] were calculated from the following equations:

$$B.\ D, (g/cm3) = W1/ (W1–W2) \times 1 \quad (7)$$

$$A.\ P, \% = (W1 – W3)/ (W1–W2) \times 100 \quad (8)$$

Where, W1, W2 and W3 are the saturated, suspended and dry weights, respectively.

Then, the compressive strength (CS) of the various hardened cement pastes[41,42] was measured using a suitable Piston as follows:

$$CS = L\ (KN)/Sa\ (cm^2)\ KN/m^2 \times 102\ (Kg/cm^2)/10.2\ (MPa) \quad (9)$$

Where L is the load taken, Sa is the surface area. Thereafter, about 10 grams of the broken specimens from the determination of compressive strength were first well ground, dried at 105°C for 30 min. and then were placed in a solution mixture of 1:1 methanol: acetone to stop the hydration.[43-45] The kinetics of hydration in terms of chemically combined water and free lime contents were also measured at each hydration age on the basis of ignition loss at 1000°C for 30 minutes soaking. About one gram of the sample was placed inside a crucible and first dried at 105°C for 24 hours, and then the crucibles were placed into a furnace.[45-47] The chemically-combined water content (CWn) at each hydration age was determined as follows:

$$CWn, \% = W1\text{-}W2/W2 \times 100 \quad (10)$$

Where, CWn, W1 and W2 are combined water content, weight of sample before and after ignition, respectively.

The free lime content (FLn) of the hydrated samples pre-dried at 105°C for 24h was also determined. About 0.5g sample +40 ml ethylene glycol → heating to about 20 minutes without boiling. About 1–2 drops of pH indicator were added to the filtrate and then titrated against freshly prepared 0.1N HCl until the pink colour disappeared. The 0.1 N HCl was prepared using the following equation: Where, Wn, W1 and W2 are combined water content, weight of sample before and after ignition, respectively. The free lime content of the hydrated samples pre-dried at 105°C for 24h was also determined. About 0.5 g sample + 40 ml ethylene glycol → heating to about 20 minutes without boiling. About 1–2 drops of pH indicator were added to the filtrate and then titrated against freshly prepared 0.1 N HCl until the pink colour disappeared. The 0.1 N HCl was prepared using the following equation:

$$V1 = N \times V2 \times W\ (7) \times 100/D \times P \times 1000 \quad (11)$$

Where, V1 is the volume of HCl concentration, V2 is the volume required, N is the normality required, W is the equivalent weight, D is the density of HCl concentration and P is the purity (%). The heating and titration were repeated several times until the pink colour did not appear on heating. The free lime content[32,14,43,45,48] was calculated from the following relation:

$$FLn, \% = (V \times 0.0033/1) \times 100 \quad (12)$$

Where, FLn and V are the free lime content and the volume of 0.1 N HCl taken on titration, respectively.

The SEM microscopy was done for some selected samples by using JEOL–JXA–840 electron analyzer at accelerating voltage of 30 KV. The fractured surfaces were fixed on Cu-kα stubs by carbon paste and then coated with a thin layer of gold.

Table 4. Chemical composition of GW in comparison with GbfS, SF, PFa, SCBA, SDA and SFSA.

Materials Oxides	GW	GbfS	SF	PFa	SCBA	SDA	SFSA
SiO_2	70.31	36	90.9	59.2	70.83	66.17	63.83
Al_2O_3	2.46	12	1.1	25.6	9.21	4.35	6.68
Fe_2O_3	0.26	1	1.5	2.9	1.95	2.36	2.79
CaO	8.69	38	0.7	1.1	8.16	10.06	5.46
MgO	3.62	----	0.8	0.3	1.32	4.41	6.23
Na_2O	12.52	0.3	----	0.2	0.12	0.08	0.24
K_2O	1.06	-----	-----	0.9	1.65	0.12	1.17
SO_3	----	8.11	0.4	0.3	1.47	0.30	1.11
P_2O_5	----	2.16	----	0.14	----	0.46	----
MnO	----	1.31	----	1.05	----	2.19	----
LOI	----	1.0	3.0	1.4	6.91	0.84	3.35

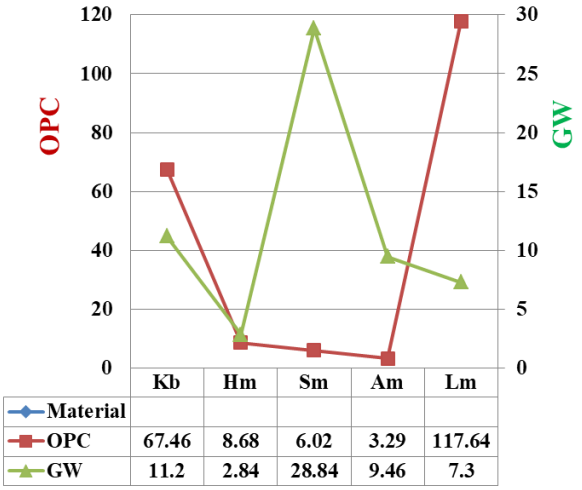

Fig. 4. Physical properties of the OPC and GW materials.

3. Results and Discussions

3.1. Chemical composition of glass powder and cement

The chemical composition of GW in comparison with some pozzolanic materials is shown in Table 4. According to ASTM C618, 2015a,[49] the sum of SiO_2+Al_2O_3 + Fe_2O_3 requirement for a standard pozzolana is 70% which is more or less that of GW samples. The standard also sets maximum limit of SO_3 and Loss on Ignition (LOI) as 4% and 10%, respectively. As shown in Table 4, the SO_3 content of GW sample was found well below the acceptable limit, whereas LOI was negligible. Therefore, the GW powder is expected to be as a pozzolanic material in the cementitious system.

3.2. Physical properties

The physical properties of the used OPC and GW samples are listed in Table 5, and plotted in Fig. 4. The hydration modulus (Hm) of either OPC or GW samples is almost the same, whereas the basicity coefficient and lime modulus (Lm) of the OPC are higher than those of GW, but the silica modulus (Sm) and alumina modulus (Am) of GW are much higher than those of OPC. The relationship between the blaine surface area, density and specific gravity of the used OPC and GW samples is represented in Fig. 5. The surface area or fineness and also the density of GW are higher than those of OPC, while its specific

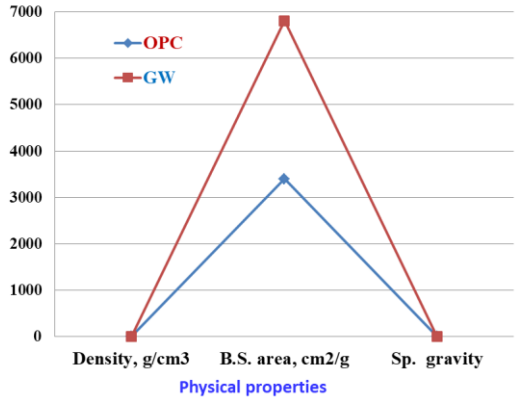

Fig. 5. Relationship between Density, Blaine surface area and specific gravity of OPC and GW samples.

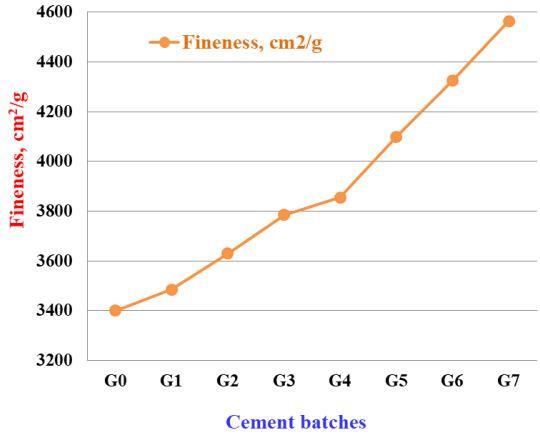

Fig. 6. Relationship between the fineness of the different cement batches containing GW.

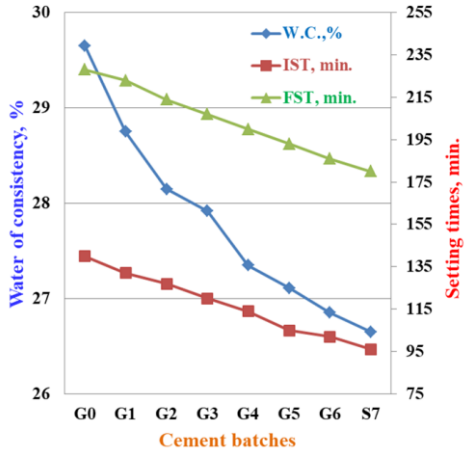

Fig. 7. Water of consistency and setting times of the various cement pastes (G0-G7).

gravity is lower. The data shown in Tables 4 and 5 confirmed that the GW could be used as a mineral admixture for cement pastes, mortars or even concretes.[15,48,49] The relationship between the surface area or fineness of the OPC (G0) and the various cement batches incorporated GW (G1-G7) is represented in Fig. 6. It is clear that as the GW content increased in the cement mix, the surface area or fineness of the whole mix increased too as shown in Table 3 and Fig. 5. This is mainly due to the presence of nanoparticles of GW.

Table 5. Physical properties of the used OPC and GW samples.

Property / Material	Kb	Hm	Sm	Am	Lm	Density, g/cm^3	Blaine Fineness, cm^2/g	Specific gravity
OPC	67.46	8.68	6.02	3.29	117.64	2.7213	3400	3.14
GW	11.20	2.84	28.84	9.46	7.30	2.7546	6810	2.86

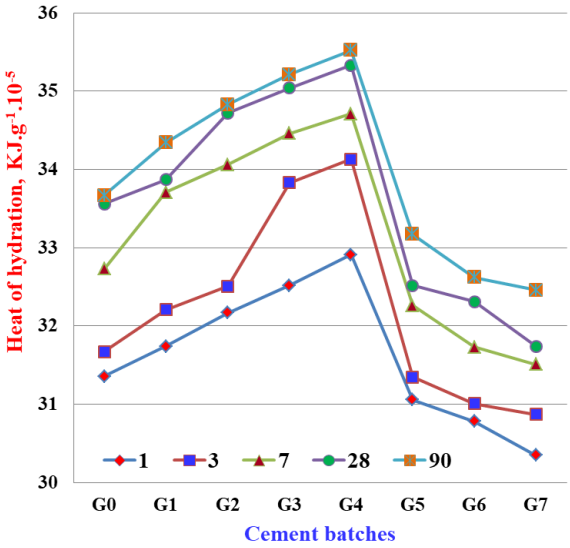

Fig. 8. Heat of hydration of the various cement pastes (G0-G7) hydrated up to 90 days.

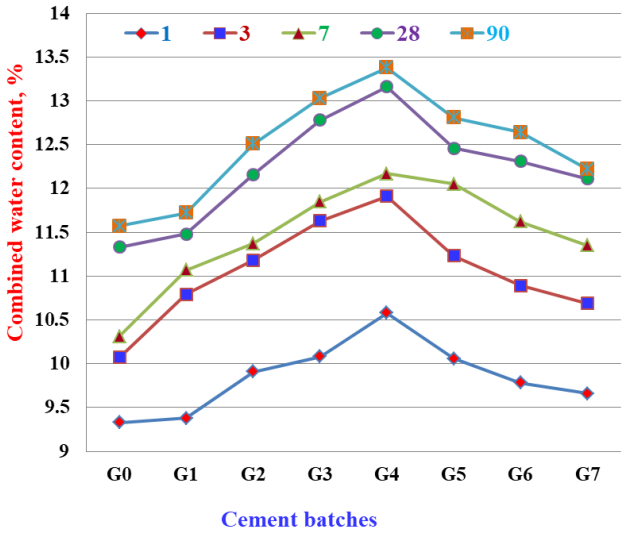

Fig. 9. Combined water contents of the various cement pastes (G0-G7) hydrated up to 90 days.

3.3. Water of consistency and setting times

Fig. 7 illustrates the water of consistency and setting times (initial and final) of the OPC (G0) and the various cement pastes containing GW (G1-G7). It is obvious that the water of consistency decreased the GW content increased. This is essentially attributed to the gradual deficiency of the main cementing material of the cement which is responsible for the hydration process in the presence of water.[12,13,21,34] On the other hand, the setting times also decreased with GW content. This is mainly due to the reason mentioned before.[24,27,33,44] The GW only reacted with the released Ca $(OH)_2$ from the hydration of cement portion to form additional CSH. This will decrease the free lime content.

3.4. Heat of hydration

The heat of hydration of the various cement pastes containing GW (G0-G7) is graphically represented as a function of hydration times for 1, 3, 7, 28 and 90 days in Fig. 8. Results illustrated that as soon as the various cement powders become in contact with water, the heat of hydration of all cement pastes was generally increased as the hydration time proceeded up to 90 days which was the same trend for all cement pastes. This is mainly due to the increase of the rate of hydration of cement pastes. This was followed by the release of heat.[32,40,49,50] Moreover, the rate of the released heat of hydration sharply enhanced at early ages up to 7 days. This is essentially attributed to the activation effect of the hydration reaction mechanism of C_3S by the very fine GW particles. At later ages (28-90 days), the rate of hydration reaction as well as the evolved heat of hydration also increased but slightly. This may be due to the activation action mechanism of β-C_2S by the fine GW particles.[34,43]

The heat of hydration increased as the GW content increased only up to 12 wt% GW (G1-G4), but with any further increase (G5-G7) lower values of heat of hydration were exhibited than those of the blank (G0) were recorded. This was contributed to the dilution effect of the main binding material (OPC), and the retardation effect of the higher quantity of GW at the expense of the OPC portion.

3.5. Combined water contents

The chemically combined water contents of the different cement pastes containing GW (G0-G7) are represented as a function of cement batches in Fig. 9. For all cement pastes, the combined water content increased as the hydration time progressed up to 90 days. This is principally contributed to the hydration of the main cement phases, especially C_3S, C_3A and C_4AF at early ages of hydration up to 7 days, whereas β-C_2S often hydrates at later ages from 28 days onward.[32,33,40] The combined water contents slightly increased as the GW content increased only up to 12 wt%, and then suddenly decreased sharply with further increase of GW almost at all hydration times, i.e. the cement blends G1, G2,G3 and G4 containing 3, 6, 9 and 12 wt% GW, respectively are slightly higher than those of the pure OPC (G0). This is primarily due to the activation effect of the nanosilica of the glass,[51-54] and moreover to the pozzolanic reactivity of GW through which the constituents of GW can react with the resulting Ca $(OH)_2$ from the hydration of C_3S at early stages of hydration and β-C_2S at later stages to produce addition CSH. Whereas, the bound water contents of G4, G6 and G7 are becoming lower than those of the control mix (G0). This may be due to that the higher amounts of GW hindered and be an obstacle for the hydration of the phases of the cement (G0), or the deficiency of the main hydrating material is the main reason for the decrease of combined

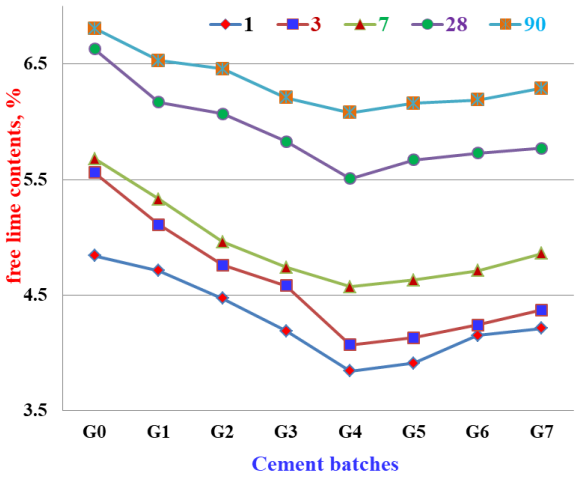

Fig. 10. Free lime contents of the various cement pastes (G0-G7) hydrated up to 90 days.

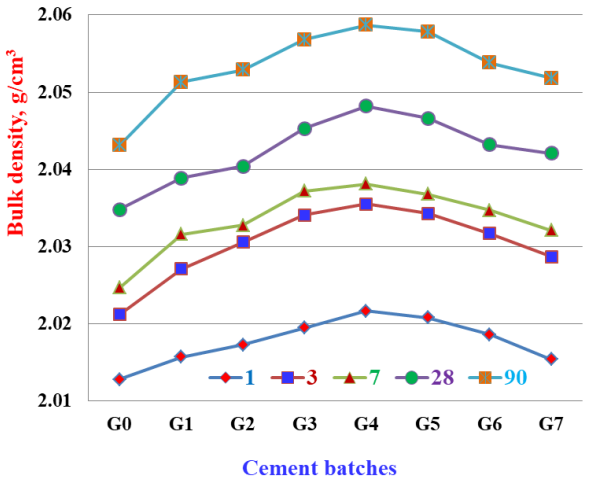

Fig. 11. Bulk density of the various cement pastes (G0-G7) hydrated up to 90 days.

water.[1,32,36,52,53] Accordingly, it can be concluded that the optimum addition of GW does not exceed 12 wt% because the higher amounts of GW is undesirable due to its adverse effect, i.e. the higher quantity of GW must be avoided because it may be hindered the hydration of cement phases. However, the combined water contents of G5, G6 and G7 are still higher than those of the blank (G0) as shown from Fig. 9.

3.6. Free lime content

Fig. 10 indicates the free lime contents of the various cement mixes (G0-G7) hydrated up to 90 days as a function of cement batches. Generally, the free lime contents of the control cement pastes (G0) were gradually increased with the hydration ages up to 90 days indicating an enhancement in the rate of hydration.[32,39] This is mainly due to the hydration process of calcium silicate phases (C_3S and C_2S) of the cement as follows:

$$3\ C_3S + 6\ H_2O \rightarrow C_3S_2H_3 + 3\ Ca(OH)_2 \quad (13)$$

$$2\ \beta\text{-}C_2S + 4\ H_2O \rightarrow C_3S_2H_3 + Ca(OH)_2 \quad (14)$$

But, as the GW content increased in the cement mixes (G1-G7), the free lime content decreased only up to 12 wt % (G4). With further increase of GW in the cement batch (G5-G7), the free lime contents started to increase gradually as the hydration ages progressed till reach to 90 days. However, the free lime contents seemed to be lower than those of the control (G0) at all hydration periods. The increase is due to the normal hydration process of the cement phases, while the decrease is due to the activation power of glass and its pozzolanic reactions between the active nanosilica of GW and the resulting $Ca(OH)_2$ from the hydration of C_3S at early ages and β–C_2S at later ages of hydration in presence of water. In the cement mixes (G1-G4), the rate of hydration improved and enhanced than in the blank (G0) at all hydration periods. This is certainly attributed to activation effect occurred by GW and also its pozzolanic reactivity with the free lime released by the cement.[52,53] The increase of free lime contents recorded by G5-G7 cement pastes decreased the rate of hydration. This is due to the lack of the essential hydrating material because the higher amount of GW hinders the rate of

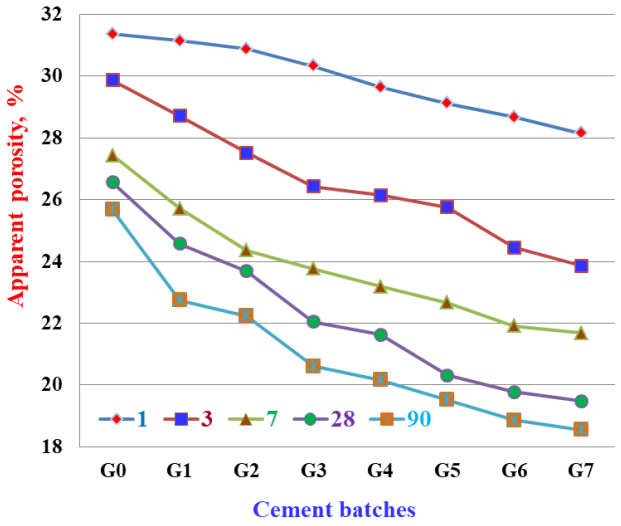

Fig. 12. Apparent porosity of the various cement pastes (G0-G7) hydrated up to 90 days.

hydration.[51-54] The obtained results proved that the GW acts as a pozzolanic material at all ages of hydration. So, the higher amounts of GW must be avoided due to its adverse effect on the physical and chemical properties of the cement.[50, 55-59]

3.7. Bulk density and apparent porosity

Figs. 11 and 12 demonstrate the graphs of the bulk density and apparent porosity of the various cement pastes (G0-G7) versus the cement batches. Generally, the bulk density of the various cement mixes increased as the hydration time progressed up to 90 days, while the apparent porosity decreased.[32,39] This is mainly contributed to that as the dry cement batches become in contact with water the hydration process begins to produce CSH and/or CAH, which soon deposited in the pore structure of samples leading to a decrease in the porosity and an increase of bulk density. As the hydration time proceeds, the formed hydration products increased too. This reflected positively on the bulk density, i.e. the bulk density increased, while the apparent porosity decreased.[21,22,52] The bulk density of the cement mixes (G1-G4) gradually increased only up to

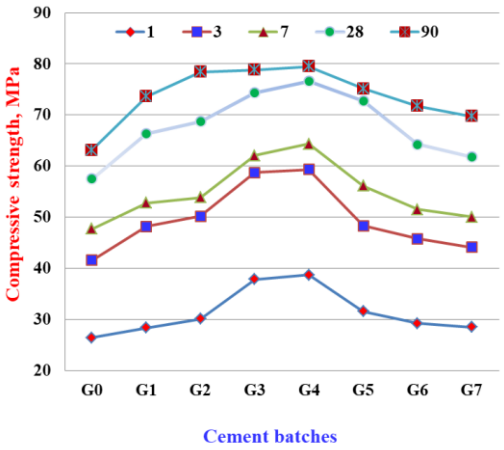

Fig. 13. Compressive strength of the various cement pastes (G0-G7) hydrated up to 90 days.

12 wt% (G4), whereas the apparent porosity decreased, i.e. the bulk density of cement blends G1-G4 is slightly higher than those of the blank (G0). This is evidently due to the formation of additional CSH and/or CAH due to the pozzolanic reactions of GW with the constituents of cement through which the constituents of GW can react with the Ca $(OH)_2$ resulting from the hydration of C_3S at early stages of hydration and β-C_2S at later stages to produce additional CSH and/or, and this is beside the normal hydration process of cement phases.[7,19-21,60] With further increase of GW (> 12 wt %), i.e. G5-G7, the BD started to decreased while the apparent porosity increased at all hydration times due to that the higher quantity of GW may obstruct and hinder the hydration process, i.e. it affects negatively and decrease the rate of hydration, but it slightly benefits as a filler.[7,22,24,29,37,46,60] Hence, the incorporation of large amounts of GW at the expense of the used OPC (G0) is undesirable. That is because it was not sufficient for inducing the reaction of cement with nanosilica of GW. So, it could be concluded that the GW is so beneficial to cement that it helps with the hydration process as a pozzolanic material and also as a filling agent.

3.8. Compressive strength

The w/c ratio of cement pastes and/or concrete affects the workability, which in turn affects the strength of cement pastes, mortars and/or concrete, i.e. the decrease of w/c-ratio results in an increase of workability accompanied by an increase in the strength of the hardened cement pastes, and the opposite is right.[32,39,60] Fig. 13 represents the graphs of the compressive strength (CS) of the various cement pastes (G0-G7) versus the cement batches and hydrated up to 90 days. The compressive strength gradually improved and enhanced as the hydration period proceeded up to 90 days. This is mainly attributed to the formation of CSH and/or CAH that precipitated into the pore structure of the hardened cement samples. This results in a decrease in the pore system and an increase in the bulk density. This improved and enhanced the compaction of the prepared samples, besides the good dispersion by the used admixture and the good compaction during casting which in turn reflected positively on the compressive strength, As a result, the compressive strength increased.[29,31,36,53] The CS also enhanced as the GW content increased at all hydration times only up to 12 wt%

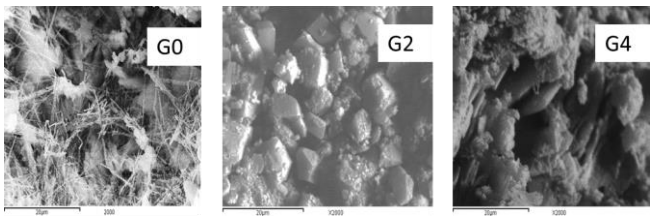

Fig. 14. The SEM microscopy of G0, G2 and G4 samples hydrated up to 28 days.

GW (G$). This is essentially due to the activation effect and formation of more CSH that is resulting from the pozzolanic reactions of nanosilica and nanoalumina of GW with the free lime evolved from the hydration of C_3S and β–C_2S of cement to produce cubic crystals of hydrogarnet ($C_3A.\ S_2.\ H_n$) as follows:-

$$Al_2O_3 + SiO_2 + Ca\ (OH)_2 \rightarrow C_3A.\ S_2.\ H_n \qquad (15)$$

On the other side, the decrease of free lime improves the physical, chemical and mechanical properties of the hardened cement pastes and therefore the CS improved and enhanced.[34,37,39,54,60] Also, this would be led to the segmentation of large capillary pores and nucleation sites due to the continuous deposition of hydration products (CSH from the normal hydration of cement phases and additional CSH from the pozzolanic reactions of GW with the released free lime.[42,47,52-55] By further increase of GW > 12 wt%, the CS values were suddenly decreased. The is due to the fact that the replacing of GW at the expense of the essential cementitious material of the cement and the higher amount of GW stand as an obstacle against the normal hydration of cement phases. So, the rate of hydration declined and accordingly, this should be reflected negatively on the CS.[39-42,60] However, the values of CS are still higher than those of the blank (G0) at all hydration ages (Fig. 12). The cement mix (G4) recorded the highest values of CS, whereas that of G7 exhibited the lowest. On this basis, the cement batch containing 12 % GW is the optimum cement batch. Hence, the GW does not only improve the various characteristics of the OPC, but from an economical point of view, it also reduces the cost of the very expensive OPC production.

3.9. Scanning electron microscopy

The SEM microscopy of G0, G2, G4 hydrated up to 28 days is shown in Fig. 14. The ettringite phase is clearly detected in G0 as needles-like crystals (A). Blocks structure and aggregates of CSH are seen with G2. Sheets or masses of CSH and/or CAH are formed with G4. In addition, spots of free lime are well detected in G0 and G2 samples with variable rates, but they are disappeared in G4 sample.

4. Conclusions

Concerning the findings of the laboratory test results, the following overall conclusions could be obtained:-

- As the nano-glass waste particles (GW) content increased in the cement batch, the fineness of the whole batches increased too.

- The water of consistency of the blank (G0) was 29.65%, and the initial and final setting times were 140 and 228 minutes. These values tended to gradually diminish or decrease with the incorporation of GW due to the presence of Na-lignosulphonate admixture, which it is a superplasticizer that reduces largely the mixing water.
- Generally, the heat of hydration, chemically combined water content, bulk density and compressive strength improved and increased gradually with the hydration ages up to 90 days. With the increase of GW content, these properties enhanced only up to 12 wt % (G4), and then decreased suddenly with its further increase.
- The free lime content of the blank (G0) and also the various cement pastes (G1-G7) increased as the hydration time proceeded up to 90 days. But with the incorporation of GW, the free lime contents are becoming lower than those of the blank.
- On contrast, the apparent porosity were diminished and reduced with the replacing up to 12 % GW (G4), and then raised and enhanced onward with further increase of > 12 wt % GW.
- The improving and enhancing of all properties could be achieved by the pozzolanic reactions leading to reduce Ca (OH)2 which is coming from the hydration of C3S and β–C2S phases of the cement, and by enhancing the precipitation sites of hydration products. Moreover, the activating and filling effects of the nano silica of the GW initiated these properties.
- The addition of 12 % GW (G4) to Portland cement could be applied without any adverse effects on the physical, chemical and mechanical properties of Portland cement. Therefore, it was selected to be the optimum batch.
- The incorporation of the Na-lignosulphonate admixture is the mean cause responsible for the modification and improving most of the physical, chemical and mechanical properties of the hardened cement pastes.
- The SEM microscopy showed the ettringite phase in the blank sample (G0), but disappeared in the samples containing glass waste (G2 and G4), which are replaced by sheets and/or blocks of CSH.

Acknowledgements

The author wishes to express his deep thanks to National Research Centre for helping to obtain materials, processing, preparing, molding and measuring all of the obtained data of the study, and moreover for financial assistance.

Conflicts of Interest

The authors declare no conflict of interest.

References

1 Darweesh H.H.M. Ceramic Wall and Floor Tiles Containing Local Waste of Cement Kiln Dust—Part I: Densification Parameters. *Am. J. Civ. Eng. Archit*., 2015, **2**, 35–43. [Link]
2 Darweesh H.H.M; Wahsh M.M.S.; Negim E.M. Densification and Thermomechanical Properties of Conventional Ceramic Composites Containing Two Different Industrial Byproducts. *Am. Eurasian J. Sci. Res.*, 2012, **7**, 123-130. [Link]
3 Phonphuak N.; Kanyakam S.; Chindaprasirt P. Utilization of Waste Glass to Enhance Physical Mechanical Properties of Fired Clay Brick. *J Clean. Prod*., 2016, **112**, 3057–3062. [CrossRef]
4 Hojamberdiev M.; Eminov A.; Xu Y. Utilization of Muscovite Granite Waste in the Manufacture of Ceramic Tiles. *Ceram. Int*., 2011, **37**, 871–876. [CrossRef]
5 Nuttawat K.; Jaimasith M.; Thiemsorn W. Fabrication of Ceramic Floor Tiles from Industrial Wastes. *Suranaree J. Sci. Technol*., 2013, **21**, 65–77. [Link]
6 Furlanin E.; Maschio S. Mechanical Properties and Microstructure of Fast Fired Tiles Made with Blends of Kaolin and Olivine Powders. *Ceram. Int*., 2013, **39**, 9391–9396. [CrossRef]
7 Kim K.; Kim K.; Hwang J. Characterization of Ceramic Tiles Containing LCD Waste Glass. *Ceram. Int.,* 2016, **42**, 7626–7631. [CrossRef]
8 Ke S.; Wang Y.; Pan Z.; Ning C.; Zheng S. Recycling of Polished Tile Waste as a Main Raw Material in Porcelain Tiles. *J. Clean. Prod*., 2016, **115**, 238–244. [CrossRef]
9 Amin S.K.; Sibak H.A.; El-Sherbiny S.A.; Abadir MF. An Overview of Ceramic Wastes Management in Construction. *Int. J. Appl. Eng*., 2016, **11**, 2680–2685. [Link]
10 Amin S.K.; Abdel-Hamid E.M.; El-Sherbiny S.A.; Sibak H.A.; Abadir M.F. The Use of Sewage Sludge in the Production of Ceramic Floor Tiles. *HBRC J*., 2017, **14**, 309–315. [CrossRef]
11 Darweesh H.H.M. Recycling of Glass Waste in Ceramics-Part I: Physical, Mechanical and Thermal Properties. *SN Appl. Sci.*, 2019, **1**, 1274. [CrossRef]
12 Imbabi M.S.; Carrigan C.; McKenna S. Trends and Developments in Green Cement and Concrete Technology. *Int. J. Sustain. Built Environ*., 2012, **1**, 194–216. [CrossRef]
13 Darweesh H.H.M. Geopolymer Cements From Slag, Fly Ash and Silica Fume Activated with Sodium Hydroxide and Water Glass. *Interceram. - Int. Ceram. Rev*., 2017, **6**, 226-231. [CrossRef]
14 Darweesh H.H.M. Effect of the Combination of Some Pozzolanic Wastes on the Properties of Portland cement Pastes. *IIC*, 2005, **808**, 298-311.
15 Darweesh H.H.M. Setting, Hardening and Strength Properties of Cement Pastes with Zeolite Alone or in Combination with Slag. *Interceram- Int. Ceram. Rev.,* 2012, **1**, 52-57. [Link]
16 Heikal M. Effect of Temperature on the Physic-Mechanical Properties of Homra Pozzolanic cement Pastes. *Cem. Conc. Res*., 2000, **11**, 1836-1839. [CrossRef]
17 Chusilp N.; Jaturapitakkul C.; Kiattikomol K. Utilization of Bagasse Ash as a Pozzolanic Material in Concrete. *Constr. Build. Mater*., 2009, **23**, 3352–3358. [CrossRef]
18 Darweesh H.H.M.; Abu-El-Suoud M.R. Influence of Sugarcane Bagasse Ash on the Properties of Portland cement Pastes. *Indian J. of Engineering*, 2019, **16**, 252-266. [Link]
19 Islam G.M.S.; Islam M.M.; Akter A.; Islam M.S. Green Construction Materials-Bangladesh Perspective. In: Proceedings of the International Conference on Mechanical Engineering and Renewable Energy 2011, (ICMERE2011) 22–24 December 2011, Chittagong, Bangladesh (ID-063). [Link]
20 Detwiler R.; Bhatty J.I.; Bhattacharja S. Supplementary Cementing Materials for Use in Blended Cements. Research and Development Bulletin Rd112t, Portland cement Association, Skokie, Illinois, USA, 1996. [Link]
21 Rashed A.M. Recycled Waste Glass as Fine Aggregate Replacement in Cementitious Materials based on Portland cement. *Constr. Build. Mater*., 2014, **72**, 340–357. [CrossRef]
22 Ryou J.; Shah S.P.; Konsta-Gdoutos M.S. Recycling of Cement Industry Wastes by Grinding Process. *Adv. Appl. Ceram*., 2006, **105**, 274–279. [CrossRef]

23 Binici H.; Aksogan O.; Cagatay I.H.; Tokyay M.; Emsen E. The Effect of Particle Size Distribution on the Properties of Blended Cements Incorporating GGBFS and Natural Pozzolan (NP). *Powder Technol*., 2007, **177**, 140–147. [CrossRef]
24 Nassar R.U.D.; Soroushian P. Strength and Durability of Recycled Aggregate Concrete Containing Milled Glass as Partial Replacement for cement. *Constr. Build. Mater*., 2012, **29**, 368–377. [CrossRef]
25 Byars E.; Meyer C.; Zhu H.Y. Use of Waste Glass for Construction Products: Legislative and Technical Issues. In: Dhir R.K.; Newlands M. D.; Halliday J.E. (Eds.), Recycling and Reuse of Waste Materials. Thomas Telford Ltd., London, United Kingdom, 2003, 827–838. [Link]
26 Matos A.M.; Sousa-Coutinho J. Durability of Mortar using Waste Glass Powder as cement Replacement. *Constr. Build. Mater*., 2012, **36**, 205–215. [CrossRef]
27 Nassar R.U.D.; Soroushian P. Field Investigation of Concrete Incorporating Milled Waste Glass. *J. Solid Waste Technol. Manage*., 2011, **37**, 307–319. [CrossRef]
28 Andreola F.; Barbieri L.; Lancellotti I.; Leonelli C.; Manfredini T. Recycling of Industrial Wastes in Ceramic Manufacturing: State of Art and Glass Case Studies. *Ceram. Int*., 2016, **42**, 13333–13338. [CrossRef]
29 Kim K.; Kim K.; Hwang J. LCD Waste Glass as a Substitute for Feldspar in the Porcelain Sanitary W`are Production. *Ceram. Int*., 2015, **41**, 7097-7102. [CrossRef]
30 Sonjida M.; Ahsan M.; Hamid A.; Ahmed S. Effect of Waste Glass Powder on Physico-Mechanical Properties of Ceramic Tiles. *Bangladesh J. Sci. Res*., 2011, **24**, 169–180. [CrossRef]
31 Phonphuak N.; Kanyakam S.; Chindaprasirt P. Utilization of Waste Glass to Enhance Physical Mechanical Properties of Fired Clay Brick. *J. Clean Prod*., 2016, **112**, 3057–3062. [CrossRef]
32 Hewlett P.C.; Liska M. Lea's Chemistry of Cement and Concrete, 5th ed., Edward Arnold Ltd., London, England, 2017.
33 Darweesh H.H.M.; Abo El-Suoud M.R.; Saw Dust Ash Substitution for Cement Pastes-Part I. *Amer. J. Constr. Build. Mater.*, 2017, **2**, 1-9. [Link]
34 Darweesh H.H.M. Characteristics of Portland cement Pastes Blended with Silica Nanoparticles. *Chem. J.*, 2020, **5**, 1-14. [Link]
35 Darweesh H.H.M.; Abo El-Suoud M.R. Palm Ash as a Pozzolanic Material for Portland cement Pastes. *Chem. J.*, 2020, **4**, 72-85. [Link]
36 Topçu I.B.; Ateşin Ö. Effect of High Dosage Lignosulphonate and Naphthalene Sulphonate based Plasticizer Usage on Micro Concrete Properties. *Constr. Build. Mater.*, 2016, **120**, 189–197. [CrossRef]
37 ASTM-C187-86. Standard Test Method for Normal Consistency of hydraulic Cement, 1993, 148-150.
38 ASTM-C191-92. Standard Test Method for Setting Time of Hydraulic Cement, 1993, 866-868.
39 Neville A.M. Properties of Concrete, 5th Ed, Longman Essex (UK), 2011. [Link]
40 Darweesh H.H.M.; Nagieb A. Hydration and micro-structure of Portland/Calcined Bentonite Blended Cement Pastes. *Indian J. Chem. Technol.*, 2007, **14**, 301-307. [Link]
41 ASTM- C170-90. Standard Test Method for Compressive Strength of Dimension Stone", 1993, 828-830.
42 ASTM-C109M. Standard Test Method for Compressive Strength of Hydraulic Cement Mortars (Using 2-in. Or [50-mm] Cube Specimens), Annual Book of ASTM Standards. ASTM International, West Conshohocken, PA, 2013.
43 ASTM C39. Standard Test Method for Compressive Strength of Cylindrical Concrete Specimens. ASTM International, West Conshohocken, USA, 2016.
44 Mohammed T.U.; Ahmed T.; Apurbo S.M.; Mallick T.A.; Shahriar F.; Munim A.; Awal AA. Influence of Chemical Admixtures on Fresh and Hardened Properties of Prolonged Mixed Concrete. *Adv. Mater. Sci. Eng.*, 2017, 1-11. [CrossRef]
45 Karim M.R.; Zain M.F.M.; Jamil M. Strength of Mortar and Concrete as Influenced by Rice Husk Ash: A Review. *World Appl. Sci. J.*, 2012, **19**, 1501-1513. [Link]
46 Siddique R. Properties of Self-Compacting Concrete Containing Class F Fly Ash. *Mater. Des*., 2011, **32**, 1501–7. [CrossRef]
47 Darweesh H.H.M. Utilization of Perlite Rock in Blended Cement-Part I: Physicomechanical Properties. *Direct Res. J. Chem. Mater. Sci.*, 2014, 2354-4163. [Link]
48 Echart A.; Ludwig H.M.; Stark J. Hydration of the Four Main Portland cement Clinker Phases. *Zement-Kalk-Gips*, 1995, **48**, 443-452.
49 ASTM C618a. Specification for Coal Fly Ash and Raw or Calcined Natural Pozzolan for Use in Concrete. ASTM International, West Conshohocken, USA, 2015.
50 Heikal M.; Ali AI.; Ismail M.N.; Awad S.; Ibrahim N.S. Behavior of Composite Cement Pastes Containing Silica Nano-Particles at Elevated Temperature. *Const. Build. Mater*., 2014, **70**, 339-350. [CrossRef]
51 Aleem S.A.E.; Heikal M.; Morsi W.M. Hydration Characteristic, Thermal Expansion and Microstructure of Cement Containing Nano-Silica. *Const. Build. Mater*., 2015, **59**, 151-160. [CrossRef]
52 Darweesh H.H.M.; Abo-El-Suoud M.R. Quaternary Cement Composites Containing Some Industrial By-products to Avoid the Environmental Pollution. *EC Chem.*, 2015, **2**, 78-91. [Link]
53 Darweesh H.H.M. Mortar Composites Based on Industrial Wastes. *Int. J. Mater. Lifetime*, 2017, **3**, 1-8. [Link]
54 Sadiqul Islam G.M.; Rahman M.H.; Kazi N. Waste Glass Powder as Partial Replacement of Cement for Sustainable Concrete Practice. *Int. J. Sustain. Built Environ*., 2017, **6**, 37–44. [CrossRef]
55 Amin M.; Abu El-Hassan K. Effect of using Different Types of Nano Materials on Mechanical Properties of High Strength Concrete. *Constr. Build. Mater*., 2015, **80**, 116–124. [CrossRef]
56 Stefanidou M.; Papayianni I. Influence of Nano-SiO_2 on the Portland cement Pastes. *Compos. Part B-Eng*., 2012, **43**, 2706–2710. [CrossRef]
57 Nazari A.; Riahi S.; Riahi S.; Shamekhi S.F.; Khademno A. Influence of Al_2O_3 Nanoparticles on the Compressive Strength and Workability of Blended Concrete. *J. Am. Sci.*, 2010, **6**, 6-9. [Link]
58 Givi A.N.; Rashid S.A.; Aziz F.N.A.; Salleh M.A.M. Experimental Investigation of the Size Effects of SiO_2 Nano-particles on the Mechanical Properties of Binary Blended Concrete. *Compos. Part B: Eng.*, 2010, **41**, 673-677. [CrossRef]
59 Ibrahim N.S.; Heikal M.; Ismail M.N. Physico-mechanical, Microstructure Characteristics and Fire Resistance of cement Pastes containing Al_2O_3 Nano-particles. *Const. Build. Mater*., 2015, **91**, 232-242. [CrossRef]
60 Rashad M.A. A Brief on High-volume Class F Fly Ash as cement Replacement – A Guide for Civil Engineer. *Int. J. Sustain. Built Environ*., 2015, **4**, 278–306. [CrossRef]